Available online at www.sciencedirect.com

ScienceDirect

www.elsevier.com/locate/jes

JES JOURNAL OF ENVIRONMENTAL SCIENCES

www.jesc.ac.cn

Seasonal variations of soil bacterial communities in *Suaeda* wetland of Shuangtaizi River estuary, Northeast China

Xuwang Zhang[1,*], *Zhe Ji*[1], *Yating Shao*[1], *Chaochen Guo*[1], *Hao Zhou*[1], *Lifen Liu*[1,2], *Yuanyuan Qu*[2]

[1] *Key Laboratory of Industrial Ecology and Environmental Engineering (Ministry of Education), School of Ocean Science and Technology, Dalian University of Technology, Panjin 124221, China*

[2] *Key Laboratory of Industrial Ecology and Environmental Engineering (Ministry of Education), School of Environmental Science and Technology, Dalian University of Technology, Dalian 116024, China*

ARTICLE INFO

Article history:
Received 21 December 2019
Revised 2 April 2020
Accepted 7 April 2020
Available online 5 June 2020

Keywords:
Microbial community
Suaeda
Rhizosphere
Nitrogen metabolism
Seasonal variation

ABSTRACT

Estuarine wetland is the transitional interface linking terrestrial with marine ecosystems, and wetland microbes are crucial to the biogeochemical cycles of nutrients. The soil samples were collected in four seasons (spring, S1; summer, S2; autumn, S3; and winter, S4) from *Suaeda* wetland of Shuangtaizi River estuary, Northeast China, and the variations of bacterial community were evaluated by high-throughput sequencing. Soil properties presented a significant seasonal change, including pH, carbon (C) and total nitrogen (TN), and the microbial diversity, richness and structure also differed with seasons. Canonical correspondence analysis (CCA) and Mantel tests implied that soil pH, C and TN were the key factors structuring the microbial community. *Gillisia* (belonging to Bacteroidetes) and *Woeseia* (affiliating with Gammaproteobacteria) were the two primary components in the rhizosphere soils, displaying opposite variations with seasons. Based on PICRUSt (Phylogenetic Investigation of Communities by Reconstruction of Unobserved States) prediction, the xenobiotics biodegradation related genes exhibited a seasonal decline, while the majority of biomarker genes involved in nitrogen cycle showed an ascending trend. These findings could advance the understanding of rhizosphere microbiota of *Suaeda* in estuarine wetland.

Introduction

Estuarine wetland is the transitional interface between land and sea, linking terrestrial with marine ecosystems. The wetland is characterized by rich biodiversity, high biological productivity and plentiful ecosystem services. Shuangtaizi River (also known as Liao River) estuary wetland, the largest estuarine wetland in high latitude China, is located downstream of Liao River and north of Bohai Sea (40°45′00″-41°5′54″N, 121°28′24.58″-121°58′27″E) (Yuan et al., 2017). The red halophyte *Suaeda heteroptera* is an annual pioneer plant widespread in intertidal zone of Shuangtaizi River estuary, which starts to grow in April with light red and matures in autumn with deep red. Thousands of acres of *Suaeda* form the famous landscape, Red Beach, in Panjin, China, developing into valuable eco-tourism resources. The Red Beach is essential

* Corresponding author.
E-mail: zhangxw@dlut.edu.cn (X. Zhang).

https://doi.org/10.1016/j.jes.2020.04.012
1001-0742/

to the preservation of migratory birds, providing the feeding and breeding habitats for numbers of waterfowls (Wang et al., 2010). Meanwhile, *Suaeda* can also assimilate multiple metal ions (Cu, Hg and Pb) (He et al., 2016; Li et al., 2019b) and capture excess nutrients and pollutants (petroleum, chemical oxygen demand (COD) and NH_4^+-N) (Li et al., 1999; He et al., 2019), which are crucial for wetland restoration and remediation.

The rhizosphere microbes can play vital roles in such processes through interactions with plants (Fester et al., 2014). Meanwhile, the structure and composition of bacterial community can be mediated by the complex physicochemical properties of soils (Hu et al., 2019). The pH is often observed with high influences on abundance and diversity of bacterial community in soils (Bahram et al., 2018; An et al., 2019). Other important factors affecting the assembly of bacterial communities in wetland soils include nutrients (NH_4^+-N, total phosphorus (TP) and NO_2^--N) (Su et al., 2018; Hu et al., 2019; Li et al., 2019a), dissolved oxygen (DO) (Wang et al., 2013; Zheng et al., 2014), salinity (Lv et al., 2016) and contaminants (petroleum, aromatics and metals) (Tian et al., 2014; Xie et al., 2017). It is well established that rhizosphere bacterial communities can also vary with time during the growth of plants (İnceoğlu et al., 2010; Philippot et al., 2013). However, the characteristics and variations of rhizosphere microbiota of *Suaeda* are currently less described. The rhizosphere of *Suaeda* in intertidal coastal soils of Gujarat, India, was characterized by high abundances of Gram-negative bacteria, total bacteria and actinomycetes (Chaudhary et al., 2015, 2017). Furthermore, the *Suaeda* wetland in Shuangtaizi River estuary was found to be rich in aromatics-degrading, sulfur-oxidizing and denitrifying bacteria, which could participate in the biogeochemical cycling and bioremediation in estuarine wetland (Zhang et al., 2019). Further comprehensive research on seasonal distribution and floatation of bacterial communities in *Suaeda* rhizosphere soils can enrich the understanding of microbial ecology in estuarine wetland.

In this study, the seasonal variations of rhizosphere microbiota in *Suaeda* wetland of Shuangtaizi River estuary, Northeast China, were evaluated based on high-throughput sequencing. The diversity, structure and metabolic function of bacterial communities were analyzed, and the potential impacts of soil properties on microbial communities were also examined.

1. Materials and methods

1.1. Sampling

This study was carried out in an intertidal zone of Shuangtaizi River estuary. Parallel sampling of rhizosphere soils was undertaken in triplicate, and the soils were sampled at the same site (40°53′29″N, 121°46′25″E) in four seasons: spring (S1; May 5, 2018), summer (S2; July 15, 2018), autumn (S3; September 23, 2018) and winter (S4; December 7, 2018) (Appendix A Fig. S1). The sampling time corresponded roughly to the different growth stage of *Suaeda*, i.e., young-plant (S1), fast-growing (S2), maturation (S3) and senescence (S4) stage. Soils attached to the roots (5–10 cm depth) were placed in plastic sheets by shovels, and each replicate contained approximately 50 g (fresh weight) soils pooled from several sampling points. The samples were transported in ice bags (4°C) and delivered to the laboratory within 12 hr. Then, each soil sample was divided into two parts: one used for chemical analysis was stored at 4°C, and the other for DNA extraction was stored at −80°C.

1.2. Soil chemical analysis

After air-dried at room temperature, the pH of soil samples was measured in a 1:10 soil:water (*m*/*V*) mixture by a FE20 pH-meter (Mettler Toledo, Switzerland), and a Vario EL cube element analyzer (Elementar Analysensysteme, Germany) was used to determine the contents of carbon (C), nitrogen (TN) and sulfur (S) in soils. The concentrations of TP, NO_3^--N, NO_2^--N and NH_4^+-N were determined spectrophotometrically using the protocols described previously (Su et al., 2018; Zhang et al., 2019). Results were expressed as mean ± SD ($n = 3$), and statistical significance between sampling seasons was examined by one-way ANOVA with a Tukey post hoc test. Pearson correlation tests were conducted in R software (v2.15.3). The data with $P < 0.05$ were considered significant.

1.3. Bacterial community analysis

The genomic DNA of the rhizosphere soils was extracted with the conventional CTAB/SDS method. The amplicons of bacterial 16S rRNA V3-V4 fragments were subjected to sequencing by Thermofisher Ion S5^{TM}XL platform at Novogene

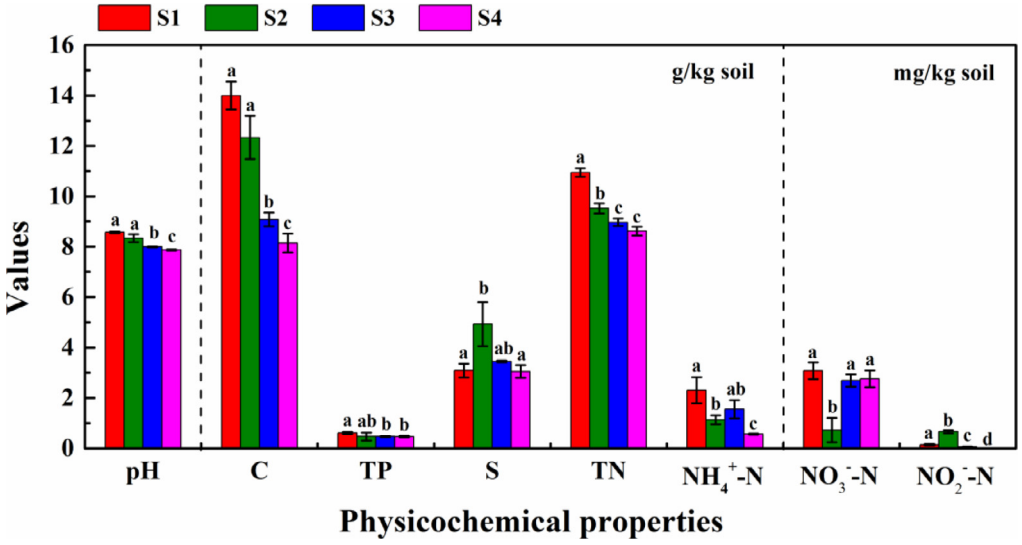

Fig. 1 – Physicochemical properties of the rhizosphere soils in different seasons (S1: spring; S2: summer; S3: autumn; S4: winter). Statistic differences between different sampling seasons are denoted by different letters (one-way ANOVA, $P < 0.05$).

Table 1 – Pearson correlation coefficient matrix between various soil properties.

Soil properties	pH	C	TP	S	TN	NH_4^+-N	NO_3^--N	NO_2^--N
pH	1.00							
C	0.95***	1.00						
TP	0.30	0.32	1.00					
S	0.28	0.22	−0.07	1.00				
TN	0.87***	0.88***	0.63*	−0.04	1.00			
NH_4^+-N	0.62*	0.63*	0.55	−0.18	0.75**	1.00		
NO_3^--N	−0.11	−0.18	0.05	−0.87***	0.09	0.31	1.00	
NO_2^--N	0.42	0.50	−0.08	0.76**	0.19	−0.04	−0.88***	1.00

* $P < 0.05$, ** $P < 0.01$ and *** $P < 0.001$.
C: carbon; TP: total phosphorus; S: sulfur; TN: total nitrogen.

Corporation (Beijing, China). After treatment of sequencing data, the sequence analysis was carried out by UPARSE program (v7.0.1001) (Edgar, 2013) to generate operational taxonomic units (OTUs) (≥ 97% similarity). SILVA132 database (Quast et al., 2012) was used for taxonomic annotation based on Mothur algorithm (Schloss et al., 2009) with a confidence cutoff of 0.8–1.0. The alpha diversity indices were calculated by Qiime program (v1.9.1) (Caporaso et al., 2010), including observed OTUs, Chao1, Shannon (H), Pielou's evenness (J) and Good's coverage. Beta diversity, like non-metric multidimensional scaling (NMDS), hierarchical cluster analysis, principal components analysis (PCA) and permutational multivariate analysis of variance (Adonis), was analyzed by R software (v2.15.3). Pearson correlation tests, canonical correspondence analysis (CCA) and Mantel tests were also conducted in R software (v2.15.3). The prediction of bacterial metabolic functions was carried out by PICRUSt (Phylogenetic Investigation of Communities by Reconstruction of Unobserved States, v1.0.0) and annotated by KEGG (Kyoto Encyclopedia of Genes and Genomes) (Langille et al., 2013). Circos plots were generated online (http://circos.ca/) to visualize the genomic data. The data of high-throughput sequencing have been deposited in NCBI Sequence Read Archive under the BioProject number PRJNA591043.

2. Results and discussion

2.1. Physicochemical properties of soils

The soil properties for each sampling time are shown in Fig. 1, and significant seasonal changes were observed. The soils were generally in alkaline conditions (pH 7.87–8.57), and the pH decreased gradually from S1 to S4. The soil pH was probably associated with precipitation, which annually increased from January to July (S2) and then decreased to December (S4) in Panjin. The abundant rainwater in S1 and S2 could promote the leaching and dissolving of salts, resulting in higher pH (Rathore et al., 2017). The plant root activities might also have an impact on soil pH. Previous study showed that soil pH of *Suaeda* wetlands in Yellow River Estuary decreased from summer to autumn, probably due to the decreasing level of *Suaeda* root activities (Wang et al., 2015). Pearson correlation analysis indicated that pH presented strong positive correlations with C, TN and NH_4^+-N ($P < 0.05$, Table 1), suggesting that pH could significantly affect the nutrients in soils (Kemmitt et al., 2006). The C and TN contents showed similar patterns, which decreased from S1 to S4 with a C/N ratio ranging from 0.97 to 1.20. A positive relationship between C and TN was observed ($P < 0.001$, Table 1), implying that the carbon and nitrogen compounds in the rhizosphere soils could be input from the same resources (Su et al., 2018). Soil carbon and nitrogen were supposed to act as a source of plant nutrients, and they could be absorbed by roots and translocated to the aboveground part during the growth of salt marsh plant (Shao et al., 2013). Thus, the growth of *Suaeda* from S1 to S3 could result in the decrease of C and TN in soils. TP concentration was detected in the range of (0.47 ± 0.03) to (0.61 ± 0.04) g/kg soil with the highest content observed in S1, which was also positively correlated with TN ($P < 0.05$, Table 1). Plenty of S was detected with relatively high concentration, particularly in S2, which was positively associated with NO_2^--N ($P < 0.01$, Table 1) but inversely related to NO_3^--N ($P < 0.001$, Table 1). NH_4^+-N with a decreasing tendency from S1 to S4 was the dominant constituent of

Table 2 – Summary of sequencing data and alpha diversity indices of microbial communities*.

Index	S1	S2	S3	S4
Shannon index	6.38 ± 0.55 a	7.79 ± 0.66 ab	8.64 ± 0.19 b	8.27 ± 1.01 ab
Pielou's evenness index	0.62 ± 0.05 a	0.73 ± 0.06 ab	0.80 ± 0.01 b	0.76 ± 0.08 ab
Chao1	1583 ± 230 a	2012 ± 136 ab	2054 ± 85 ab	2130 ± 123 b
OTU number	1303 ± 123 a	1712 ± 94 b	1808 ± 77 b	1836 ± 222 b
Good's coverage	(98.80±0.29)%	(98.63±0.21)%	(98.73 ± 0.26)%	(98.67 ± 0.09)%
Number of phyla	34	33	39	41
Number of classes	41	44	46	47
Number of orders	89	97	97	99
Number of families	163	176	174	178
Number of genera	332	370	363	384

* Statistic differences between different sampling seasons are denoted by different letters (one-way ANOVA, $P < 0.05$).

inorganic nitrogen, which was consistent with the founding in the tidal freshwater wetlands of Yellow River Delta (Li et al., 2019a). NO_3^--N contents were almost similar except in S2, while NO_2^--N showed a reverse pattern (P <0.001, Table 1), which was more abundant in S2. The lower amount of NH_4^+-N and NO_3^--N in S2 could be caused by the leaching and runoff losses during rainy season (Rathore et al., 2017).

2.2. Sequencing statistics and diversity of bacterial communities

A total of 782,883 clean sequences were obtained from 12 soil samples by high-throughput sequencing, and the OTU numbers ranged from 1266 to 1988 with Good's coverage over 98% across all samples, suggesting that the observed OTUs could be a representative of the bacterial communities (Table 2). Rarefaction curves and the Chao1 values demonstrated that the taxa richness increased from S1 to S4 with seasons (Appendix A Fig. S2 and Table 2). The Shannon index (H) varied from 6.381 to 8.643, and the accompanying Pielou's evenness index (J) was in the range of 0.617 to 0.799 (Table 2), which showed that the bacterial biodiversity underwent a sharp increase from S1 to S3 (P <0.05) and then slightly decreased in S4 (P > 0.05). The changes in community biodiversity could be attributed to the plant growth and temperature variation. In spring (S1), *Suaeda* began to grow, and the root exudates could promote the growth of microbes in soils. Then the biodiversity of soil communities continued to increase with the growth of *Suaeda* in summer (S2), but the high temperature would have certain inhibitory effects. In autumn (S3), the suitable temperature and mature plants steadily increased the diversity of microbes. When *Suaeda* entered senescence stage (S4) in winter with low temperature, the soil bacterial diversity decreased. Similarly, the bacterial communities in the rhizosphere of different potato cultivars were influenced by plant growth stage, and the total bacterial abundance increased with the plant growth and decreased until senescence stage for most cultivars (İnceoğlu et al., 2010).

NMDS plot visualized the variations of bacterial communities at OTU level (Fig. 2a). The results showed that the samples displayed seasonal changes, leading to the formation of three clusters. S1 and S2 were clearly separated from each other, while S3 and S4 drifted away and clustered together. Similar variation tendency was also observed from PCA and hierarchical cluster analysis (Fig. 2b and c). Adonis analysis evaluated the differences in microbial communities between seasons (Appendix A Table S1). The results showed that S1 was clearly distinct from the others (P <0.05), and S2 also differed from S3 (P <0.05), indicating that the microbial communities varied significantly from spring to autumn. On the contrary, there was no significant difference between S3 and S4 (P > 0.05), suggesting that the bacterial community structure at autumn and winter was similar.

CCA assessed the linkages between soil properties and bacterial community structure (Fig. 2d). The ANOVA test identified that pH (F = 2.35, P <0.05), C (F = 2.55, P <0.05) and TN (F = 2.69, P <0.01) were the most significant variables in the assembly of bacterial communities. Mantel tests were consistent with the CCA results, and three environmental parameters could have a profound influence in structuring bacterial community assemblages, i.e., pH (r = 0.30, P <0.05), C (r = 0.39, P <0.05) and TN (r = 0.42, P = 0.01) (Appendix A Table S2). The structure and composition of rhizosphere microbial communities could be governed by the physicochemical properties of soils (Philippot et al., 2013). Soil pH was one of the principle factors controlling the microbial community assembly, which showed strong influences in topsoil (Bahram et al., 2018), arable soils (Rousk et al., 2010) and river sediments (Liu et al., 2015). In our previous study, pH was also found to be the most important factor in bacterial community assembly of reed and *Suaeda* wetlands (Zhang et al., 2019). Therefore, the seasonal variations in *Suaeda* rhizosphere community structure could be associated with the changes in soil pH. Moreover, soil carbon and nitrogen could strongly interact with microbial communities (Deng et al., 2016), thus the changes in soil C and TN could probably induce the alterations in soil community structure. Previous studies determined that organic carbon and nitrogen had an important impact on microbial biomass in rhizosphere sediments of halophytes (Chaudhary et al., 2017), while TN was a key factor in assembly of bacterial community in river sediments (Liu et al., 2018). The influence of other soil properties, like TP and inorganic nitrogen constituents, on soil community might be small in this study, but it was still non-negligible. For instance, NH_4^+-N and available phosphorous (AP) were reported to be the important factors affecting community composition in a tidal freshwater wetland (Li et al., 2019a).

2.3. Composition and structure of bacterial community

The phylogenetic classification of sequence tags resulted in 33–41 phyla, 41–47 classes, 89–99 orders, 163–178 families and 332–384 genera (Table 2). Proteobacteria and Bacteroidetes were the two predominant phyla, covering over 77% of the classified sequences (Fig. 3a). Proteobacteria was found to be the most abundant and ubiquitous phylotype in diverse plant rhizospheres (Mendes et al., 2013), soils (Delgado-Baquerizo et al., 2018) and wetlands (An et al., 2019). Bacteroidetes with various ecological functions was also reported to inhabit the sediments, soils and water environments (Wolińska et al., 2017). Proteobacteria gradually increased in relative abundance from S1 (34.3%) to S3 (62.8%), and then decreased slightly to S4 (52.1%) (Appendix A Fig. S3). Bacteroidetes exhibited the opposite tendency, the relative abundance of which declined from S1 (52.1%) to S3 (16.6%) and subsequently rose in S4 (28.6%) (Appendix A Fig. S3). Other dominant phyla included Gemmatimonadetes (2.4%-5.3%), Actinobacteria (2.7%-4.5%), Firmicutes (1.4%-3.2%), Acidobacteria (1.4%-2.3%) and Thaumarchaeota (0.1%-1.8%). According to Pearson correlation analysis, pH, C and TN were negatively correlated with Proteobacteria but positively correlated with Bacteroidetes, which demonstrated the influences of these factors on soil community compositions. Gemmatimonadetes and Actinobacteria also exhibited significant relationships with S, NO_2^--N and NO_3^--N (P <0.05, Appendix A Table S3).

In Proteobacteria, the class level distributions showed that Gammaproteobacteria (16.2%-38.7%), Alphaproteobacteria (8.9%-13.0%) and Deltaproteobacteria (7.5%-15.0%) were the major components, which were comparable to those in soils (Delgado-Baquerizo et al., 2018) and sediments (Liu et al., 2015). The relative abundances of Gammaproteobacteria and Deltaproteobacteria increased with seasons from S1 to S3 and decreased afterward in S4, while Alphaproteobacteria showed a reverse trend (Appendix A Fig. S3). However, only Gammaproteobacteria exhibited significant correlations with pH, C and TN (P <0.05, Appendix A Table S3). Zetaproteobacteria was also found in S3 and S4, which was considered as a candidate of marine iron-oxidizing bacteria (Field et al., 2015), but it accounted for few portions (<0.1%). Betaproteobacteria was undetected in the rhizosphere soils (<0.01%), which was coincident with our previous finding that the amount of Betaproteobacteria in *Suaeda* wetland was quite low (Zhang et al., 2019).

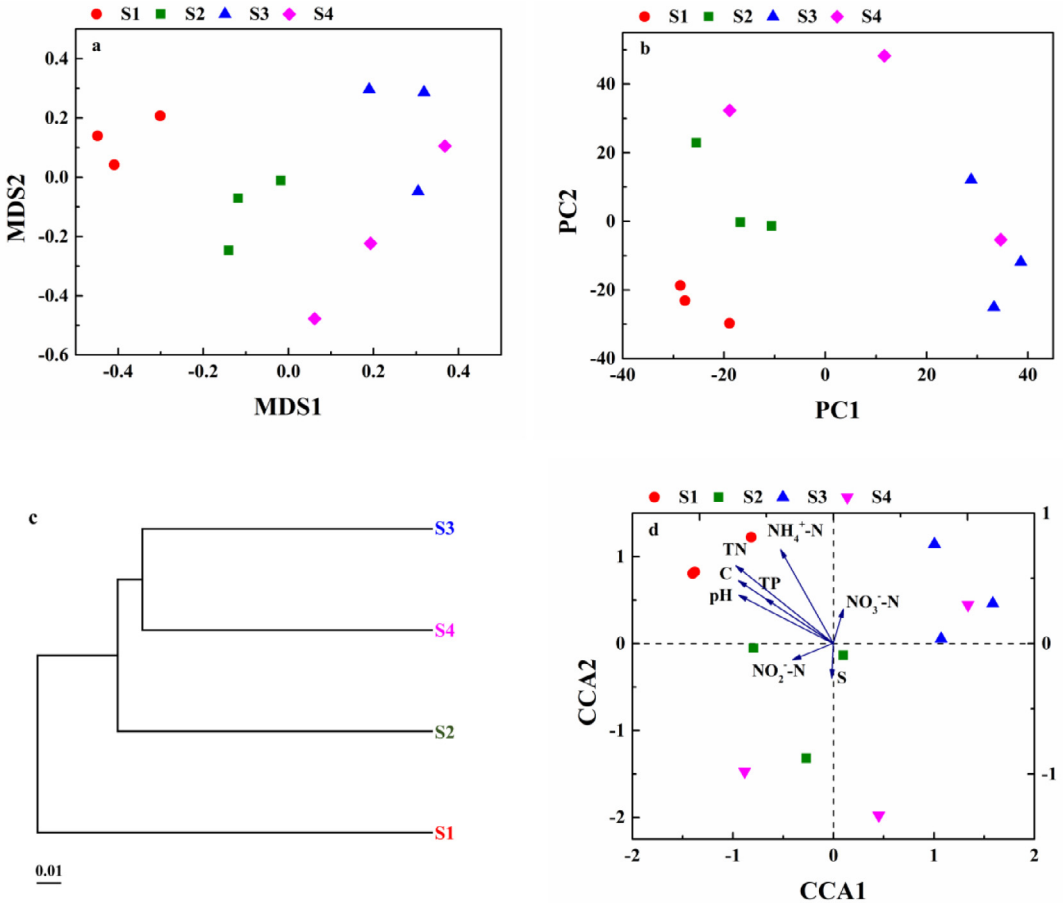

Fig. 2 – (a) Non-metric multidimensional scaling (NMDS), (b) principal components analysis (PCA) and (c) hierarchical cluster analysis reflecting the distribution of rhizosphere bacterial communities at OTU level, and (d) canonical correspondence analysis (CCA) showing the relationship between rhizosphere soil properties and bacterial community structure.

At genus level, the 20 most abundant genera (> 0.35% on average) were chosen for comparison (Fig. 3b). *Gillisia* and *Woeseia* were the two primary components in the rhizosphere soils, but they presented vastly different variations with seasons. *Gillisia*, belonging to Bacteroidetes, was the core genus in S1 with a high sequence percentage of 40.6%, but it decreased sharply to 2.3% in S3 and then recovered to 16.6% in S4 (Appendix A Fig. S3). Conversely, *Woeseia*, affiliating with Gammaproteobacteria, steadily increased from S1 (5.3%) to S3 (19.1%), becoming the predominant population, yet the relative abundance decreased in S4 (9.8%) (Appendix A Fig. S3), lower than that of *Gillisia*. Pearson correlation analysis showed that *Gillisia* was positively associated with C and TN ($P < 0.05$, Appendix A Table S4), while *Woeseia* was negatively correlated with TN ($P < 0.05$, Appendix A Table S4). *Gillisia* and *Woeseia* have been both identified in different marine environments (Roh et al., 2013; Mußmann et al., 2017). *Gillisia* was detected in the sediments of Athabasca River with a significant positive correlation with polycyclic aromatic hydrocarbons (PAHs) (Yergeau et al., 2012), which could have the potential for bioremediation of organic pollutants existing in Shuangtaizi River estuary. *Woeseia* could carry out diverse ecological functions like dissimilatory sulfur oxidation and denitrification (Mußmann et al., 2017), which could contribute a lot to biogeochemical cycling of nutrients in the estuarine wetland. *Sulfurovum, Roseovarius, Lutibacter, Fusibacter* and *Sulfitobacter* also dominated in S1 accounting for > 1.0% of the total sequences, all of which showed a positive relationship with TN ($P < 0.05$, Appendix A Table S4), but these genera subsequently declined to below 1.0%. On the other hand, *Limibacillus, Robiginitalea* and *Cetobacterium* experienced an increase from S1 to above 1.0% in S3 or S4. Based on Pearson correlation analysis, a large amount of genera showed significant positive or negative relationship with pH, C and TN ($P < 0.05$, Appendix A Table S4), which further confirmed the dominant roles of these soil properties in determining the bacterial community composition. In addition, NH_4^+-N, TP and S presented significant correlations with some genera ($P < 0.05$, Appendix A Table S4), suggesting these factors could also affect soil community structure to some extent.

2.4. *Metabolic functional analysis of bacterial community*

The metabolic functions of rhizosphere microbiota were predicted by PICRUSt program based on 16S rRNA sequencing data (Langille et al., 2013). The functional categories assigned to metabolism, genetic information processing and environmental information processing were the prevalent functions at KEGG level 1, accounting for > 78% of all sequence tags (Appendix A Fig. S4a). The most abundant functions at KEGG level 2 were amino acid metabolism and carbohydrate metabolism, which decreased in abundance from S1 to S3 and then rose up in S4 (Appendix A Fig. S4b). The functions related to membrane transport, energy metabolism and translation were also

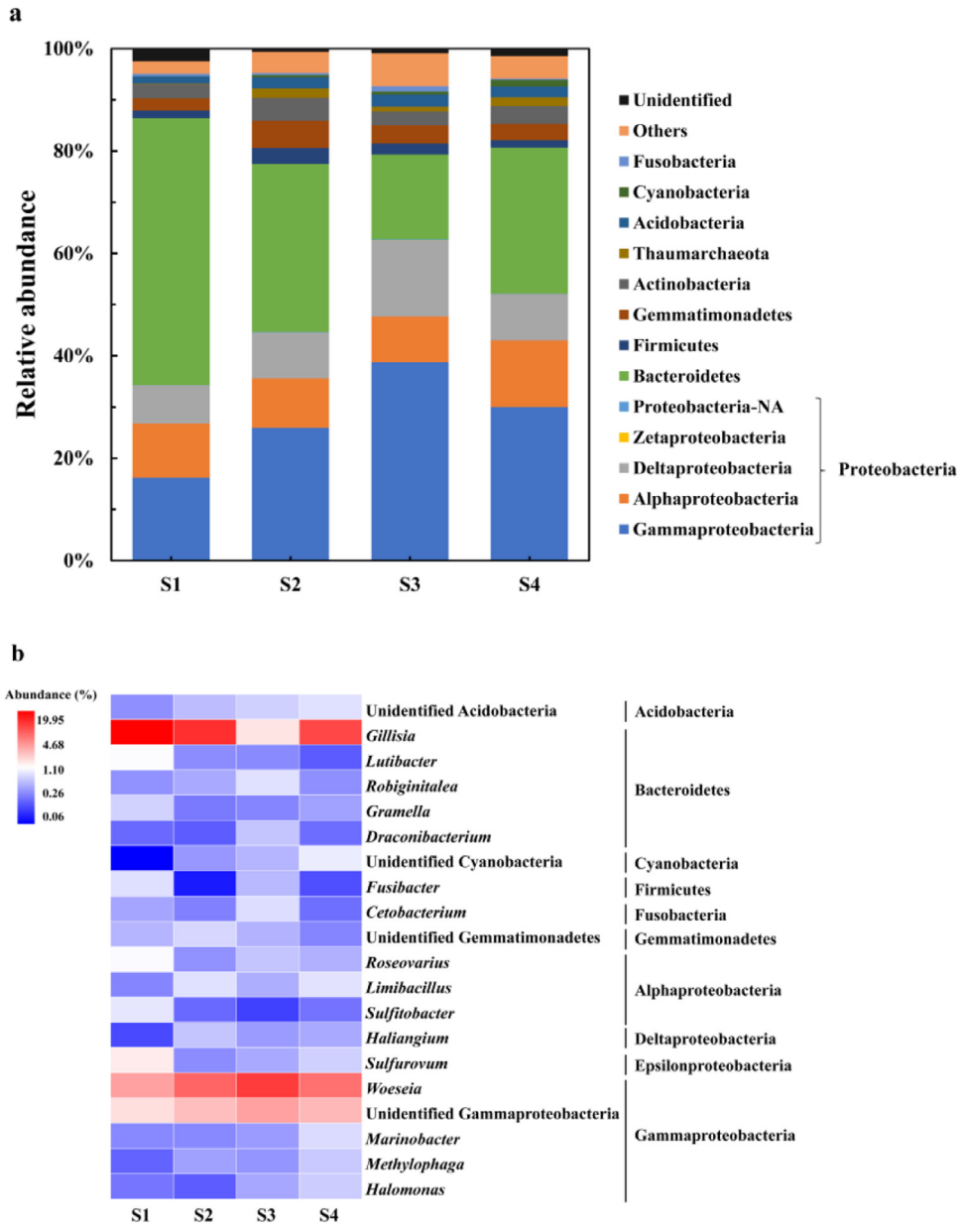

Fig. 3 – Abundances of the dominant (a) phyla and (b) genera in rhizosphere soils.

predicted with high abundance, which gradually increased in abundance from S1 to S3 and then dropped to S4 (Appendix A Fig. S4b).

Further investigation was focused on the functions relevant to xenobiotics biodegradation and nitrogen metabolism (Fig. 4). The category of xenobiotics biodegradation and metabolism exhibited a seasonal decline from S1 to S3 and then recovered in S4 (Appendix A Fig. S5). Similar variations were also observed from the dominant subcategories involved in degradation of benzoate, aminobenzoate, naphthalene, chloroalkane and chloroalkene, and drugs (Fig. 4a). Among the 20 functional categories within xenobiotics biodegradation and metabolism, only 5 of them showed different seasonal changes, such as the functions relevant to degradation of dioxin, nitrotoluene and xylene, and cytochrome P450 (Fig. 4a). These 5 functional genes increased from S1 to S3 or S4, though the gene abundances were relatively low. Pearson correlation analysis revealed that TN was the critical factor for xenobiotics biodegradation, which showed significant positive relationships with functional genes for degradation of bisphenol, DDT, drug, ethylbenzene and naphthalene, and also negatively correlated with xylene degradation gene (Appendix A Table S5). Previous studies already showed the role of nitrogen in xenobiotics bioremediation, and nitrogen amendment could be used to increase the biodegradation rates of petroleum hydrocarbons and atrazine (García-González et al., 2003; Fuentes et al., 2014). The functional profiles indicated that the rhizosphere microbiota of *Suaeda* was capable of reducing diverse nutrients and pollutants, which were crucial for the wetland restoration (Zhang et al., 2019; Bao et al., 2017).

The functions related to nitrogen metabolism at KEGG level 3 almost had no difference among the four seasons (Ap-

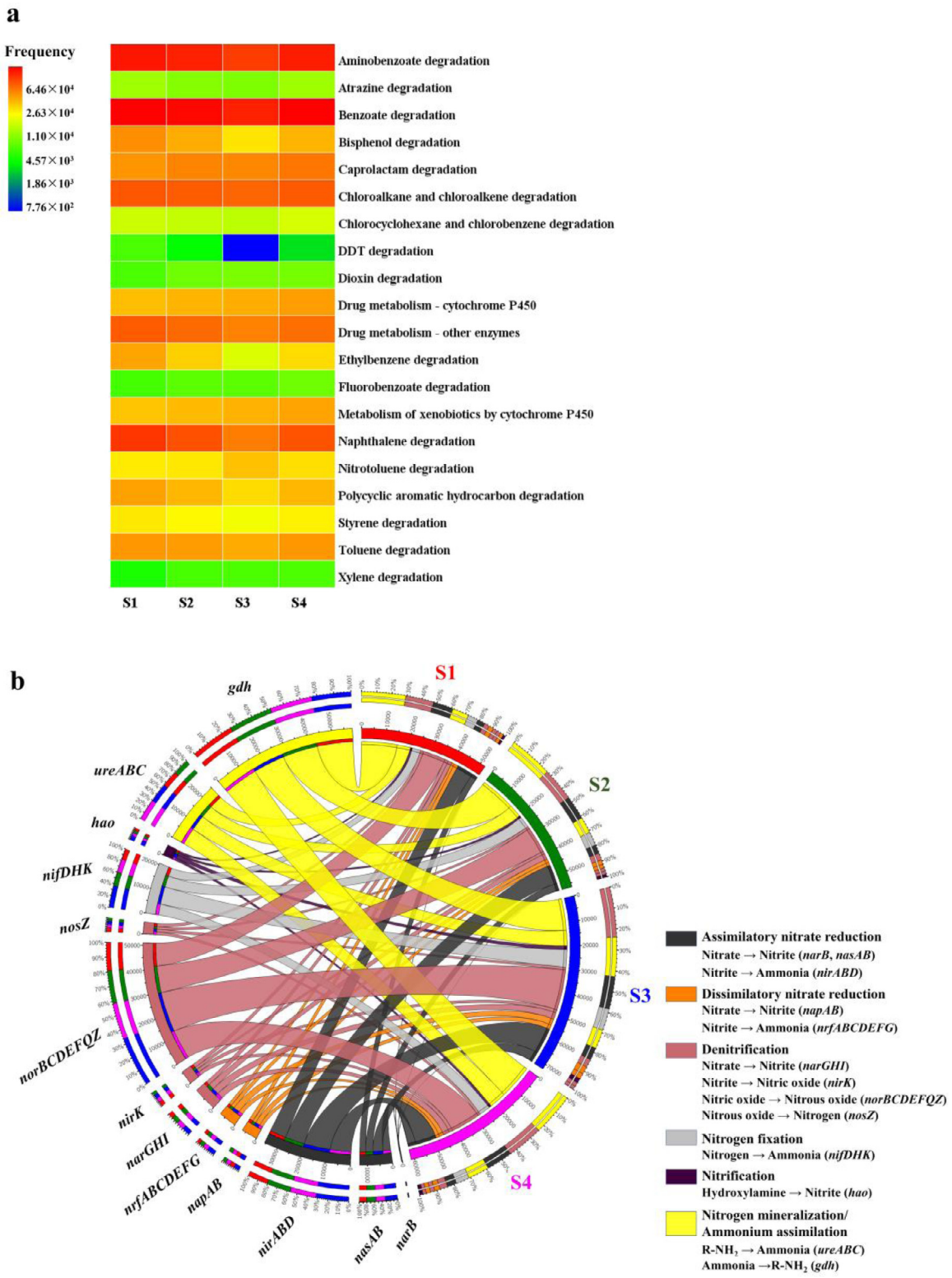

Fig. 4 – Predicted metabolic functions involved in (a) xenobiotics biodegradation and (b) nitrogen metabolism as visualized by heatmap and Circos, respectively.

pendix A Fig. S5). The functional biomarker genes relevant to nitrogen conversion were further concerned, and approximately 6 major processes involved in nitrogen cycle were detected, i.e., assimilatory nitrate reduction (ANRA), dissimilatory nitrate reduction (DNRA), denitrification, nitrogen fixation, nitrification, and nitrogen mineralization/ammonium assimilation (Fig. 4b and Appendix A Table S6) (Zehr and Kudela, 2011; Stein and Klotz, 2016; Kuypers et al., 2018). Furthermore, the majority of these biomarker genes showed a seasonal trend of ascending from S1 to S3 and then descending to S4 (Fig. 4b).

ANRA and DNRA were responsible for the reduction of nitrate to ammonia via two-step reaction: (I) nitrate → nitrite; and (II) nitrite → ammonia (Kuypers et al., 2018). The *narB* and *nasAB* (cytoplasmic nitrate reductase) genes were detected to catalyze the first step in ANRA, and the NAD(P)H-dependent nitrite reductase (*nirABD*) played the vital role in the second step. In DNRA, the periplasmic nitrate reductase (*napAB*) and formate-dependent nitrite reductase (*nrfABCDEFG*) successively took part in the reactions. The ANRA and DNRA related genes apparently increased from S1 to S3 and then decreased to S4, and ANRA accounted for higher abundances.

The rhizosphere bacterial communities could also perform the denitrification from nitrate to nitrogen. The *narGHI* genes were detected with an increase from S1 to S3, which encoded the membrane-bound nitrate reductase. The haem- (cd_1-NIR, *nirS*) and copper-containing (Cu-NIR, *nirK*) nitrite reductases were assumed to catalyze the reduction of nitrite to form nitric oxide (Jetten, 2008; Kuypers et al., 2018), but only *nirK* was observed in the rhizosphere soils. Unlike other nitrogen cycle related genes, the abundance of *nirK* showed a decrease from S1 to S3 and then restored in S4. The *norBCDEFQZ* was predicted to encode nitric oxide reductases and *nosZ* encoded nitrous oxide reductase, which were responsible for the reduction of nitric oxide via nitrous oxide to nitrogen. Furthermore, the number of *norBCDEFQZ* genes was much higher than that of *nosZ* genes, which could result in the accumulation and release of nitrogenous gas (N_2O) to the environment (Stein and Klotz, 2016). According to Pearson correlation analysis (Appendix A Table S7), the *narGHI* genes exhibited negative relations with pH, C, TP, TN and NH_4^+-N, whereas *nirK* genes were positively correlated with NO_3^--N but negatively associated with NO_2^--N, which suggested that the denitrification processes were more sensitive to the soil properties.

The rhizosphere microbiota also abounded with iron-containing nitrogenase genes (*nifDHK*), especially in S3, which contributed to the replenishment of the pool of biological available nitrogen in terrestrial environments (Kuypers et al., 2018). Although the hydroxylamine oxidoreductase genes (*hao*) were predicted with modest abundances, the bacterial ammonium monooxygenase genes (*amoABC*) were below detection, which indicated that the nitrification process was mild. The anammox related genes were also barely detected, but it still needed further demonstration with more specific molecular tools. Nevertheless, the relatively weak activities in nitrification and anammox processes could lead to the higher residual of NH_4^+-N in rhizosphere soils than NO_3^--N and NO_2^--N, which was in accord with results in wetland of Yellow River Delta (Li et al., 2019a).

The nitrogen mineralization and ammonium assimilation processes were also analyzed by targeting at urease and glutamate dehydrogenase, respectively. In soil biota, eukaryotic and prokaryotic microorganisms can assimilate ammonium and/or organic nitrogen compounds into biomass via enzymes, glutamate dehydrogenase (GDH), for instance (Zehr and Kudela, 2011; Kuypers et al., 2018). Furthermore, the soil organisms may also release organic nitrogen (e.g., urea) into the environment, which is mineralized to ammonium by heterotrophic microbes using specific enzymes (e.g., urease) (Zehr and Kudela, 2011; Kuypers et al., 2018). Herein, the urease genes (*ureABC*) were abundant in the rhizosphere soils, presenting an increasing tendency from S1 to S3. Relatively high abundances of GDH genes, such as *gudB* (EC: 1.4.1.2), *gdhA* (EC: 1.4.1.3) and *gdhA* (EC: 1.4.1.4), were detected in the rhizosphere bacterial communities, suggesting a good ability in ammonium assimilation, yet the abundances slightly decreased from S1 to S3. Overall, the rhizosphere microbiota of *Suaeda* abounded in functional genes involved in nitrogen metabolism, which was essential for the biogeochemical processes and cycling of elements in estuarine wetland.

3. Conclusions

This study revealed the seasonal variations of rhizosphere bacterial communities in *Suaeda* wetland of Shuangtaizi River estuary by high-throughput sequencing. The soil properties underwent a significant change with seasons, and pH, C and TN could greatly influence the assemblages of bacterial communities in rhizosphere soils. Proteobacteria and Bacteroidetes were predominant phyla in rhizosphere soils with *Woeseia* and *Gillisia* being the most primary genera, all of which presented a seasonal variation. Predicted by PICRUSt analysis, the microbial metabolic profiles of the rhizosphere microbiota were obtained, and 6 major processes of nitrogen metabolism were identified with an increasing shift from S1 to S3 for the majority of biomarker genes. The present study should provide insights into the characteristics and variations of *Suaeda* rhizosphere microbiota with seasonality, which may contribute to preservation and restoration of estuarine wetland.

Declaration of Competing Interest

The authors declare that they have no known competing financial interests or personal relationships that could have appeared to influence the work reported in this paper.

Acknowledgments

This work was supported by the National Natural Science Foundation of China (Nos. 31970107, 51508068) and the Fundamental Research Funds for the Central Universities (No. DUT19JC17). The authors would also like to acknowledge the support from the Undergraduate Innovation and Entrepreneurship Training Program in Dalian University of Technology.

Appendix A Supplementary data

Supplementary material associated with this article can be found, in the online version, at doi:10.1016/j.jes.2020.04.012.

REFERENCES

An, J., Liu, C., Wang, Q., Yao, M., Rui, J., Zhang, S., et al., 2019. . Soil bacterial community structure in Chinese wetlands. Geoderma 337, 290–299.
Bahram, M., Hildebrand, F., Forslund, S.K., Anderson, J.L., Soudzilovskaia, N.A., Bodegom, P.M., et al., 2018. . Structure and function of the global topsoil microbiome. Nature 560 (7717), 233–237.

Bao, Y.J., Xu, Z., Li, Y., Yao, Z., Sun, J., Song, H., 2017. High-throughput metagenomic analysis of petroleum-contaminated soil microbiome reveals the versatility in xenobiotic aromatics metabolism. J. Environ. Sci. 56, 25–35.
Caporaso, J.G., Kuczynski, J., Stombaugh, J., Bittinger, K., Bushman, F.D., Costello, E.K., et al., 2010. QIIME allows analysis of high-throughput community sequencing data. Nat. Methods 7 (5), 335–336.
Chaudhary, D.R., Gautam, R.K., Yousuf, B., Mishra, A., Jha, B., 2015. Nutrients, microbial community structure and functional gene abundance of rhizosphere and bulk soils of halophytes. Appl. Soil Ecol. 91, 16–26.
Chaudhary, D.R., Rathore, A.P., Kumar, R., Jha, B., 2017. Spatial and halophyte-associated microbial communities in intertidal coastal region of India. Int. J. Phytoremediation 19 (5), 478–489.
Delgado-Baquerizo, M., Oliverio, A.M., Brewer, T.E., Benavent-González, A., Eldridge, D.J., Bardgett, R.D., et al., 2018. A global atlas of the dominant bacteria found in soil. Science 359 (6373), 320–325.
Deng, Q., Cheng, X., Hui, D., Zhang, Q., Li, M., Zhang, Q., 2016. Soil microbial community and its interaction with soil carbon and nitrogen dynamics following afforestation in central China. Sci. Total Environ. 541, 230–237.
Edgar, R.C., 2013. UPARSE: highly accurate OTU sequences from microbial amplicon reads. Nat. Methods 10, 996–998.
Fester, T., Giebler, J., Wick, L.Y., Schlosser, D., Kästner, M., 2014. Plant-microbe interactions as drivers of ecosystem functions relevant for the biodegradation of organic contaminants. Curr. Opin. Biotechnol. 27, 168–175.
Field, E.K., Sczyrba, A., Lyman, A.E., Harris, C.C., Woyke, T., Stepanauskas, R., et al., 2015. . Genomic insights into the uncultivated marine Zetaproteobacteria at Loihi Seamount. ISME J 9 (4), 857–870.
Fuentes, S., Méndez, V., Aguila, P., Seeger, M., 2014. Bioremediation of petroleum hydrocarbons: catabolic genes, microbial communities, and applications. Appl. Microbiol. Biotechnol. 98 (11), 4781–4794.
García-González, V., Govantes, F., Shaw, L.J., Burns, R.G., Santero, E., 2003. Nitrogen control of atrazine utilization in *Pseudomonas* sp. strain ADP. Appl. Environ. Microbiol. 69 (12), 6987–6993.
He, J., Fan, X., Liu, H., He, X., Wang, Q., Liu, Y., et al., 2019. The study on *Suaeda heteroptera Kitag, Nereis succinea* and bacteria's joint bioremediation of oil-contaminated soil.. Microchem. J. 147, 872–878.
He, J., Ji, Z., Wang, Q., Liu, C., Zhou, Y., 2016. Effect of Cu and Pb pollution on the growth and antionxidant enzyme activity of *Suaeda heteroptera*. Ecol. Eng. 87, 102–109.
Hu, Y., Zhang, Z., Huang, L., Qi, Q., Liu, L., Zhao, Y., et al., 2019. Shifts in soil microbial community functional gene structure across a 61-year desert revegetation chronosequence. Geoderma 347, 126–134.
İnceoğlu, Ö., Salles, J.F., van Overbeek, L., van Elsas, J.D., 2010. Effects of plant genotype and growth stage on the betaproteobacterial communities associated with different potato cultivars in two fields. Appl. Environ. Microbiol. 76 (11), 3675–3684.
Jetten, M.S.M., 2008. The microbial nitrogen cycle.. Environ. Microbiol. 10 (11), 2903–2909.
Kemmitt, S.J., Wright, D., Goulding, K.W., Jones, D.L., 2006. pH regulation of carbon and nitrogen dynamics in two agricultural soils. Soil Biol. Biochem. 38 (5), 898–911.
Kuypers, M.M.M., Marchant, H.K., Kartal, B., 2018. The microbial nitrogen-cycling network.. Nat. Rev. Microbiol. 16 (5), 263–276.
Langille, M.G., Zaneveld, J., Caporaso, J.G., McDonald, D., Knights, D., Reyes, J.A., et al., 2013. Predictive functional profiling of microbial communities using 16S rRNA marker gene sequences. Nat. Biotechnol. 31 (9), 814–821.
Li, H., Chi, Z., Li, J., Wu, H., Yan, B., 2019a. Bacterial community structure and function in soils from tidal freshwater wetlands in a Chinese delta: potential impacts of salinity and nutrient. Sci. Total Environ. 696, 134029.
Li, H., Zheng, D., Yang, J., Wu, C., Zhang, S., Li, H., et al., 2019b. Salinity and redox conditions affect the methyl mercury formation in sediment of *Suaeda heteroptera* wetlands of Liaoning Province. Northeast China. Mar. Pollut. Bull. 142, 537–543.
Li, X., Qu, X., Wang, L., Zhang, H., Xiao, D., 1999. Purification function of the natural wetland in the Liaohe Delta. J. Environ. Sci. 11, 236–242.
Liu, S., Ren, H., Shen, L., Lou, L., Tian, G., Zheng, P., et al., 2015. pH levels drive bacterial community structure in sediments of the Qiantang River as determined by 454 pyrosequencing. Front. Microbiol. 6, 285.
Liu, T., Zhang, A.N., Wang, J., Liu, S., Jiang, X., Dang, C., et al., 2018. Integrated biogeography of planktonic and sedimentary bacterial communities in the Yangtze River. Microbiome 6 (1), 16.
Lv, X., Ma, B., Yu, J., Chang, S.X., Xu, J., Li, Y., et al., 2016. Bacterial community structure and function shift along a successional series of tidal flats in the Yellow River Delta. Sci. Rep. 6, 36550.
Mendes, R., Garbeva, P., Raaijmakers, J.M., 2013. The rhizosphere microbiome: significance of plant beneficial, plant pathogenic, and human pathogenic microorganisms. FEMS Microbiol. Rev. 37 (5), 634–663.
Mußmann, M., Pjevac, P., Krüger, K., Dyksma, S., 2017. Genomic repertoire of the Woeseiaceae/JTB255, cosmopolitan and abundant core members of microbial communities in marine sediments. ISME J. 11 (5), 1276–1281.
Philippot, L., Raaijmakers, J.M., Lemanceau, P., Van Der Putten, W.H., 2013. Going back to the roots: the microbial ecology of the rhizosphere. Nat. Rev. Microbiol. 11 (11), 789–799.
Quast, C., Pruesse, E., Yilmaz, P., Gerken, J., Schweer, T., Yarza, P., et al., 2012. The SILVA ribosomal RNA gene database project: improved data processing and web-based tools. Nucl. Acids Res. 41 (D1), D590–D596.
Rathore, A.P., Chaudhary, D.R., Jha, B., 2017. Seasonal patterns of microbial community structure and enzyme activities in coastal saline soils of perennial halophytes. Land Degrad. Dev. 28 (5), 1779–1790.
Roh, S.W., Lee, M., Lee, H.W., Yim, K.J., Heo, S.Y., Kim, K.N., et al., 2013. *Gillisia marina* sp. nov., from seashore sand, and emended description of the genus *Gillisia*. Int. J. Syst. Evol. Microbiol. 63 (10), 3640–3645.
Rousk, J., Bååth, E., Brookes, P.C., Lauber, C.L., Lozupone, C., Caporaso, J.G., et al., 2010. Soil bacterial and fungal communities across a pH gradient in an arable soil. ISME J. 4 (10), 1340–1351.
Schloss, P.D., Westcott, S.L., Ryabin, T., Hall, J.R., Hartmann, M., Hollister, E.B., et al., 2009. Introducing mothur: open-source, platform-independent, community-supported software for describing and comparing microbial communities. Appl. Environ. Microbiol. 75 (23), 7537–7541.
Shao, X., Wu, M., Gu, B., Chen, Y., Liang, X., 2013. Nutrient retention in plant biomass and sediments from the salt marsh in Hangzhou Bay estuary, China.. Environ. Sci. Pollut. Res. 20 (9), 6382–6391.
Stein, L.Y., Klotz, M.G., 2016. The nitrogen cycle.. Curr. Biol. 26 (3), R83–R101.
Su, Z., Dai, T., Tang, Y., Tao, Y., Huang, B., Mu, Q., et al., 2018. Sediment bacterial community structures and their predicted functions implied the impacts from natural processes and anthropogenic activities in coastal area. Mar. Pollut. Bull. 131, 481–495.
Tian, W., Zhao, Y., Sun, H., Bai, J., Wang, Y., Wu, C., 2014. The effect of irrigation with oil-polluted water on microbial communities in estuarine reed rhizosphere soils. Ecol. Eng. 70, 275–281.
Wang, J., Bai, J., Gao, Z., Lu, Q., Zhao, Q., 2015. Soil as levels and bioaccumulation in *Suaeda salsa* and *Phragmites australis* wetlands of the Yellow River Estuary, China.. BioMed Res. Int. 2015, 301898.
Wang, L., Liu, L., Zheng, B., Zhu, Y., Wang, X., 2013. Analysis of the bacterial community in the two typical intertidal sediments of Bohai Bay, China by pyrosequencing.. Mar. Pollut. Bull. 72, 181–187.
Wang, Y., Liu, R., Gao, H., Bai, J., Ling, M., 2010. Degeneration mechanism research of *Suaeda heteroptera* wetland of the Shuangtaizi Estuary National Nature Reserve in China.. Procedia Environ. Sci. 2, 1157–1162.
Wolińska, A., Kuźniar, A., Zielenkiewicz, U., Izak, D., Szafranek-Nakonieczna, A., Banach, A., et al., 2017. Bacteroidetes as a sensitive biological indicator of agricultural soil usage revealed by a culture-independent approach. Appl. Soil Ecol. 119, 128–137.
Xie, Y., Hong, S., Kim, S., Zhang, X., Yang, J., Giesy, J.P., et al., 2017. . Ecogenomic responses of benthic communities under multiple stressors along the marine and adjacent riverine areas of northern Bohai Sea, China. Chemosphere 172, 166–174.
Yergeau, E., Lawrence, J.R., Sanschagrin, S., Waiser, M.J., Korber, D.R., Greer, C.W., 2012. Next-generation sequencing of microbial communities in the Athabasca River and its tributaries in relation to oil sands mining activities. Appl. Environ. Microbiol. 78 (21), 7626–7637.
Yuan, X., Yang, X., Zhang, A., Ma, X., Gao, H., Na, G., et al., 2017. Distribution, potential sources and ecological risks of two persistent organic pollutants in the intertidal sediment at the Shuangtaizi Estuary, Bohai Sea of China. Mar. Pollut. Bull. 114, 419–427.
Zehr, J.P., Kudela, R.M., 2011. Nitrogen cycle of the open ocean: from genes to ecosystems. Annu. Rev. Mar. Sci. 3, 197–225.
Zhang, X., Zhang, L., Zhang, L., Ji, Z., Shao, Y., Zhou, H., et al., 2019. Comparison of rhizosphere bacterial communities of reed and *Suaeda* in Shuangtaizi River Estuary, Northeast China.. Mar. Pollut. Bull. 140, 171–178.
Zheng, B., Wang, L., Liu, L., 2014. Bacterial community structure and its regulating factors in the intertidal sediment along the Liaodong Bay of Bohai Sea, China.. Microbiol. Res. 169 (7-8), 585–592.